Tunneling Through a Tilted Tight-Binding Band

ALEXANDER ONIPKO[a] AND LYUBA MALYSHEVA[b]

[a]*Division of Physics, Luleå University of Technology, S-971 87 Luleå, Sweden*

[b]*Bogolyubov Institute for Theoretical Physics, Kiev, 03143, Ukraine*

ABSTRACT: In the single-band approximation, an explicit expression of the exponential factor, that governs tunneling through a thin crystal subjected to a constant electric field, is derived. The basic features of Wannier-Stark, Airy, and intermediate type of quantization, as they are displayed in the transmission spectrum and hence in tunneling current, are thus described analytically.

KEYWORDS: tunneling; Zener tunneling; Wannier-Stark effect; field emission; tunneling assisted by Wannier-Stark and surface electron states; resonance tunneling through a tilted band; quantum electron transport

I. INTRODUCTION

The concept of Wannier-Stark ladder (WSL) was invented by Wannier[1] forty years ago. During the last decade, it has been used particularly extensively for interpreting electric field effects in solids, supperlattices, and optically driven lattices.[2] Extensive literature also exists on the theoretical effort aimed at understanding regularities of electronic spectra in the presence of a constant electric field and their manifestation in Zener tunneling,[3] Franz-Keldysh effect,[4] and other related phenomena. In this long-term stream of publications, there are few analytical results obtained for the exactly solvable model of tilted tight-binding band.[5] On its basis, changes produced by a constant electric field in the electronic structure can be described in many important details that are characteristic of real systems.

Recently,[6] the referred model has been used to show that, coexisting in thin crystals, the Airy (surface) and Wannier-Stark (WS) (bulk) spectra are merging one into another via the spectrum region with doubled Wannier-level spacing. Also noteworthy, at voltages that are not high enough for opening the WS band, the middle part of the band spectrum is shown to form a WSL with level spacing $q\mathcal{F}$, where $\mathcal{F}$ is equal to Planck's constant times the Bloch oscillation frequency, and q (>1) can be an integer as well as a fractional number. In contrast to the canonical WSL ($q = 1$), which appears when the electrostatic potential energy exceeds the zero-field bandwidth E_{bw}^{0}, the value of q is controlled by the applied voltage in a certain manner that clearly distinguishes noncanonical WSLs.

Address for correspondence: Alexander Onipko, Department of Physics, IFM, Linköping University, S-581 83 Linköping, Sweden.Voice: +46 920 492002; fax: +46 920 491074.
alex@mt.luth.se

Ann. N.Y. Acad. Sci. 960: 143–152 (2002).

In continuation, to display electric field effects in transport-related characteristics, we shall consider tunneling through a tilted tight-binding band. This problem is, to an extent, similar to the electron transmission through a trapezoid barrier. However, classical treatments in the 1960s and later, commonly suppose the barrier capped by a free-electron spectrum. For obvious reasons, such a model prevents the possibility to describe tunneling through a WS band. The real-space tunneling through a tilted band is intimately related to the two-band effects of Zener,[7] and Franz and Keldysh.[8] This inspires for the present analysis as a necessary first step toward an understanding of those far more complicated phenomena.

II. FINITE TILTED BAND SPECTRUM

Under the influence of a constant electric field, electronic states in a finite tight-binding band are rearranged. The rearrangement depends on the magnitude of the applied voltage. There are two voltage intervals, where the field effects on electronic

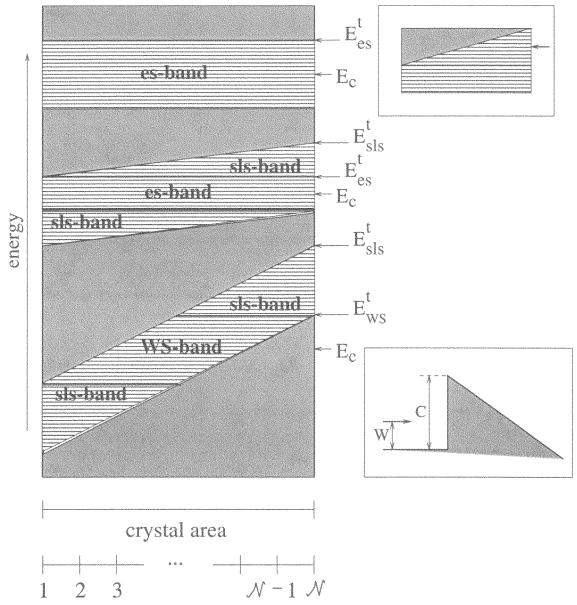

FIGURE 1. Untilted and tilted bands of electronic levels in a crystal of finite thickness. The crystal area in the direction of electric field is occupied by $\mathcal{N}$ monoatomic layers. *Shaded rectangle*, *triangle,* and *parallelogram* correspond to the extended states (*es*), surface localized states (*sls*), and Wannier-Stark (WS) bands, respectively. Index *t* (superscript) labels the highest possible energy of the respective bands: $E^t_{es} = (E^0_{bw} - \mathrm{eV})/2$, $E^t_{\mathrm{WS}} = (\mathrm{eV} - E^0_{bw})/2 = \overline{\mathrm{eV}}/2$, $E^t_{sls} = (E^0_{bw} + \mathrm{eV})/2$; E_c is the spectrum center. Classically forbidden areas are black. It is assumed that outside the crystal, any energy is accessible for incident electrons (the case of energy tuned with *sls*-band is shown in *upper inset*). *Lower inset* represents the Fowler-Nordheim model; see text for the meaning of the labels.

band states differ qualitatively. These are low voltages ($eV < E_{bw}^0$) and high voltages ($eV > E_{bw}^0$). As is seen from the tilted band diagrams shown in FIGURE 1, in the case of low voltages, there is a band of extended states (the *es* band), where electronic states are delocalized over the entire crystal thickness. Additionally, two bands of surface localized states (*sls* bands) are present in the spectrum. Within the energy interval of the upper *sls* band (because of the spectrum symmetry, we will consider only positive energies), the electronic states have a tendency to be preferably localized near the right-hand-side crystal surface. This means that the maximal amplitude of the wavefunction describing localized surface states is attained at this surface. A new feature of electronic spectrum in the case of high voltages is that instead of the *es* band, there is a band of bulk localized states, or WS band, half of which covers the energy interval $E \le (eV - E_{bw}^0)/2 \equiv \overline{eV}/2$. Further description of the electronic band structure in the presence of an electric field can be found in Ref. 6.

The region containing a band of electronic states that is tilted by a constant electric field, is supposed here to be in contact with the source and drain electrodes. In such a case, the field effects on the electronic states just outlined will influence the probability of electron tunneling between the electrodes. In what follows, we discuss the peculiarities of tunneling through a tilted band that originate from two essentially different types of electronic state quantization and that are characteristic for the surface localized and WS states. Real-space tunneling across a WS band has not been addressed so far, at least, not to our knowledge.

III. TUNNELING PROBABILITY

The Green function formalism has been proved to be an efficient tool in studies of electrical transport phenomena (see, e.g., Ref. 9 and references therein). Generally, the Green function of the whole system (i.e., a scattering region connected to leads) is required. Provided it is known, the transmission can be calculated. Except for the case of *es*-assisted tunneling, the tunneling (or transmission) probability typically contains a factor, which is decaying exponentially with the increase of the scattering region length. The exponential factor depends on the properties of the scattering region only, while the corresponding preexponential factor also includes characteristics of the leads and their interaction with the scatterer. Here, in focus is the exponential factor that reflects the strongest dependence of tunneling probability on the electron energy and electric field. It can be found without a full-scale solution of the scattering problem.

Whenever an excess electron having some kinetic energy along the electric field appears at the right(left)-hand side of the crystal, it will be transmitted to the opposite crystal side with a certain probability. The probability for an electron to tunnel through the crystal [denoted below as $T(E)$] is scaled by the ratio between squared amplitudes of the electron wavefunction at the surface atoms

$$T(E) \sim |\psi_1(E)|^2/|\psi_{\mathcal{N}}(E)|^2, \quad \textbf{(1)}$$

where indexes 1 and $\mathcal{N}$ refer to the left and right bounding surfaces of the crystal, and E stands for the *field parallel* component of the electron energy (see FIG. 1).

Due to the relationship between the Green function and eigenvectors of one and the same Hamiltonian H, the tunneling probability is readily expressible in terms of the Green function

$$T(E) \sim G^2{}_{1\mathcal{N}}(E)/G^2{}_{\mathcal{N}\mathcal{N}}(E). \tag{2}$$

The required matrix elements $G_{nn'} = (I/(EI - H)_{nn'}$, $I_{nn'} = \delta_{nn'}$, can be obtained by solving the set of equations

$$\sum_{n''=1}^{\mathcal{N}} (E\delta_{n,n''} - H_{nn''})G_{n''n'}(E) = \delta_{n,n'} \tag{3}$$

with the Hamiltonian matrix given by

$$H_{nn'} = -\mathcal{F}\left(\frac{\mathcal{N}+1}{2} - n\right)\delta_{n,n'} + \delta_{|n-n'|,1}\,. \tag{4}$$

In Eqs. (3) and (4) $n,m = \overline{1,\mathcal{N}}$, $\mathcal{F} = eFa/\beta$, e, F, and a are, respectively, the absolute value of electron charge, electric field strength, and lattice constant; the energy of electron resonance transfer between neighboring sites β serves as an energy unit; the electron site energy in zero field is set equal to zero.

Equation (3) has an exact explicit solution.[10] For the matrix elements of interest, it reads

$$G_{1\mathcal{N}}(E) = \frac{\mathcal{F}}{\pi D_{\mathcal{N}}(E)}\,, \tag{5}$$

$G_{11}(E) = -G_{\mathcal{N}\mathcal{N}}(-E)$, and

$$D_{\mathcal{N}}(E)G_{11}(E) = [J_{\mu+(\mathcal{N}-1)/2}(z)\,Y_{\mu-(\mathcal{N}+1)/2}(z) - Y_{\mu+(\mathcal{N}-1)/2}(z)\,J_{\mu-(\mathcal{N}+1)/2}(z)], \tag{6}$$

where

$$D_{\mathcal{N}}(E) = J_{\mu+(\mathcal{N}+1)/2}(z)\,Y_{\mu-(\mathcal{N}+1)/2}(z) - Y_{\mu+(\mathcal{N}+1)/2}(z)\,J_{\mu-(\mathcal{N}+1)/2}(z), \tag{7}$$

$\mu \equiv E/\mathcal{F}$, $z \equiv 2/\mathcal{F}$, and $J_\mu(z)$ and $Y_\mu(z)$ are the Bessel functions of the first and second kind, respectively.

Exactly the same set of equations as Eqs. (3), (4), and (7) has been used to classify field-effected bulk and field-induced surface states in a spatially finite tilted band.[6] Similarly, for $\mathcal{F} \ll 1$ and $\mathcal{N} \gg 1$, further analysis of the tunneling probability is based on standard approximations of Bessel functions with large arguments and small or large orders.[11] The indicated restrictions are consistent with the most realistic situations. (The opposite case of large field parameter $\mathcal{F} \geq 1$ is easily treated by perturbation theory in the small parameter $\mathcal{F}^{-1}$; it requires, however, unrealistically high applied voltages.) The particular approximation to be used depends on the energy interval. Therefore, the *sls* and WS bands are considered separately.

IV. TUNNELING THROUGH THE BAND OF SURFACE LOCALIZED STATES

For energies not too close to the *sls*-band edges, $|E_{bw}^0/2 - \mathrm{eV}/2| + \mathcal{E} < E < E_{bw}^0/2 + \mathrm{eV}/2 - \mathcal{E}$ (each of excluded $\mathcal{E}$-small intervals contains one or no electron states at all), the exact dependence of $G_{\mathcal{N}\mathcal{N}}(E)$ on the field and energy, represented in Eqs. (6) and (7), is accurately reproduced by the following relation

$$\mathcal{D}_{\mathcal{N}}(E)G_{\mathcal{N}\mathcal{N}}(E) \approx \frac{\mathcal{E}}{\pi}\frac{1}{\sqrt{\sin\xi\sinh\delta}} \times \left[\frac{1}{2}\sin\left(\frac{2}{\mathcal{E}}\Phi_\xi - \frac{\pi}{4}\right)\exp\left(-\frac{2}{\mathcal{E}}\Phi_\delta - \delta\right) + \cos\left(\frac{2}{\mathcal{E}}\Phi_\xi - \frac{\pi}{4}\right)\exp\left(\frac{2}{\mathcal{E}}\Phi_\delta + \delta\right)\right], \tag{8}$$

where $2\cosh\delta = E + \mathrm{eV}/2$, $\Phi_\delta = \delta\cosh\delta - \sinh\delta$, $2\cos\xi = E - \mathrm{eV}/2$ ($0 \le \xi \le \pi$), and $\Phi_\xi = \sin\xi - \xi\cos\xi$. Using this result in Eq. (2), we obtain

$$T(E) \sim \frac{\sin\xi\sinh\delta\exp(-2\delta)}{\cos^2\left(\frac{2}{\mathcal{E}}\Phi_\xi - \frac{\pi}{4}\right)}\exp\left(-\frac{4}{\mathcal{E}}\Phi_\delta\right). \tag{9}$$

In the same approximation, $\mathcal{D}_{\mathcal{N}}(E) \sim \cos((2/\mathcal{E})\Phi_\xi + \xi - (\pi/4))$, so that for eigenvalues satisfying equation $\mathcal{D}_{\mathcal{N}}(E) = 0$, Eq. (9) transforms into

$$T(E) \sim \frac{\exp(-2\delta)\sinh\delta}{\sin\xi}\exp\left(-\frac{4}{\mathcal{E}}\Phi_\delta\right). \tag{10}$$

Literally, the preceding relation is defined only for eigenvalues of Hamiltonian H. At these energies, approximation (10) is in excellent agreement with Eq. (2) calculated by using exact Green functions (5) and (6), as is illustrated in FIGURE 2. However, since the tunneling probability must have maxima at energy levels within the tunneling region (which will differ from H eigenvalues because of the interaction with the leads), the exponential factor in Eq. (10) may be regarded as an envelope of the transmission spectrum within the *sls*-band energy interval. This statement is confirmed by a rigorous treatment of the transmission probability, which includes coupling of the scattering region with semi-infinite leads.[12] Moreover, it turns out that in the case of identical leads and weak band-to-leads coupling, Eq. (10) gives the envelope of maxima in the transmission probability up to a factor of 4.

A. Links with Semiclassical Theory of Field Emission

It can be shown that in the continuous limit, the obtained result reconfirms an exponential factor in the Fowler and Nordheim formula[13] describing the field emission tunneling probability. This notice implies that the WS band is not yet open ($\mathrm{eV} < E_{bw}^0$). Then the top of triangular barrier is followed by the band of extended states (see FIG. 1). By analogy, in the Fowler-Nordheim (FN) model, the free electron continuous spectrum is above the barrier top, as shown in the inset in FIGURE 1.

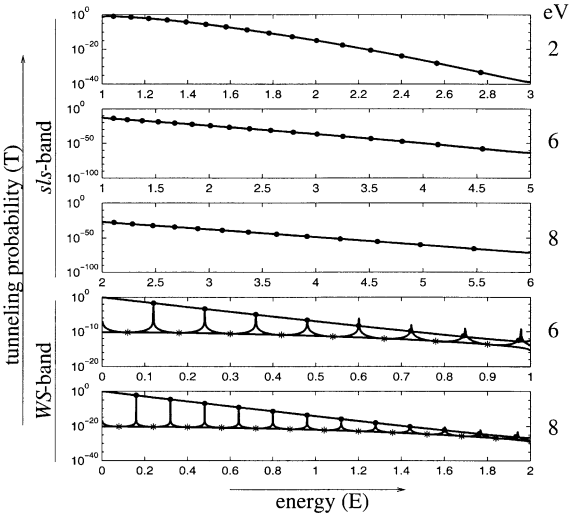

FIGURE 2. Enveloping curves of through tilted-band tunneling probability. Three upper graphs represent the *sls* band, Eq. (10). *Smooth lines* in two lower graphs correspond to maxima-envelope and minima-envelope in the WS band, Eqs. (15) and (16), respectively. Equation (2) calculated with the exact Green function gives oscillating dependence of $T(E)$. Its values at and between the WSL energies are indicated by *filled circles* and *stars*, respectively. For eV = 2 there is no WS band (the first curve from top). The second and third curves are a continuation of those depicted in the fourth and fifth graphs and marked by *circles*. In calculations, $\mathcal{N}$= 51; $\mathcal{E}$ = 0.04, 0.12, and 0.16.

To facilitate the comparison, we represent the original citation and our notations

$$T(E) \sim \exp\left[\frac{4\sqrt{2m^*}(C-W)^{3/2}}{3\hbar F}\right] \xrightarrow[\text{in our notations}} \exp\left(-\frac{4\delta^3}{3\mathcal{E}}\right) = \exp\left(-\frac{4(E-E_{es}^t)^{3/2}}{3\mathcal{E}}\right). \tag{11}$$

In Eq. (11), W is the kinetic energy of an incident electron, and C is the barrier height (see inset in FIG. 1). We emphasize that equation $\delta^2 = E - E_{es}^t$ used earlier is valid only in the continuous limit, in which case the equivalence of all three exponents in Eq. (11) is easily verified. Indeed, introducing an imaginary wavevector $i\kappa$ [in the region of triangular barrier $C - W = \hbar^2\kappa^2/(2m^*)$], making use of the β-to-m^* relation in the effective mass approximation [$\beta = \hbar^2/(2m^*a^2)$], and passing to dimensionless energy [$C - W \to (C - W)/\beta$] and wavevector ($\kappa \to \delta/a$), we arrive at

$$4\sqrt{2m^*}(C-W)^{3/2}/(3\hbar F) = 4\delta^3/(3\mathcal{E}).$$

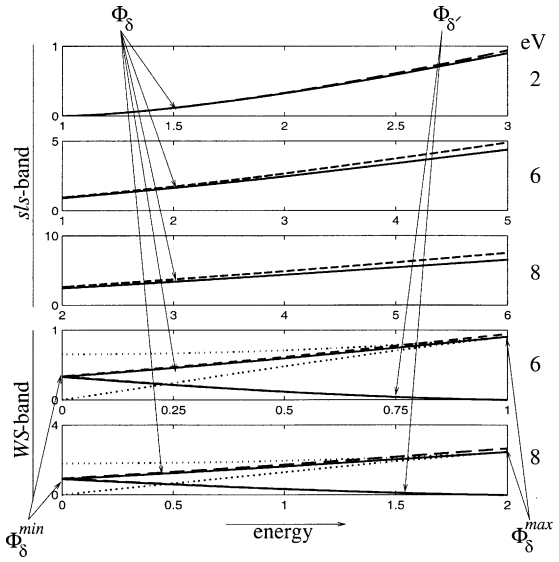

FIGURE 3. Exact (*solid lines*) and approximate (*dashed lines*) dependencies $\Phi_\delta(E)$ and $\Phi_{\delta'}(E)$. Three upper graphs correspond to *sls* band. In two lower graphs for WS band, *upper* (*lower*) *solid* and *dashed lines* represent $\Phi_\delta(E)$ $[\Phi_{\delta'}(E)]$, $3\Phi_\delta^{\min} = (\overline{eV}/2)^{3/2}$, $3\Phi_\delta^{\max} = \overline{eV}^{3/2}$. Combinations $\Phi_\pm = \Phi_\delta \pm \Phi_{\delta'}$ are plotted by *dotted lines*.

Surprisingly, to an extent, the approximation $3\Phi\delta \approx (E - E_{es}^t)^{3/2}$ used in Eq. (11) (which strictly speaking, is justified only if $E - E_{es}^t \ll 1$) turns out, in fact, to be adequate for reasonable estimates within the full *sls* band (see FIG. 3).

In spite the similarity demonstrated between the exponential factors, governing the through *sls*-band tunneling — and that appears in the FN theory — there are also major distinctions. First, the dependence of $E_{es}^t = \overline{eV}/2$ on the applied voltage is not present in the FN factor. Therefore, the actual field dependence of tunneling probability at a fixed energy, as prescribed by Eq. (10), differs substantially from that derived from the semiclassical description of tunneling through triangular[13] and trapezoid[14] barriers. Second, there is no semiclassical analogy with the purely quantum case of high voltages ($eV > E_{bw}^0$), when the WS band is open. In the latter case, for the applied potential not exceeding much zero-field bandwidth, $\overline{eV} \le E_{bw}^0$, $3\Phi_\delta \approx (E + \overline{eV}/2)^{3/2}$, so that $T(E)$ $\sim \exp[-4(E + \overline{eV}/2)^{3/2}/(3\mathcal{F})]$. In its field dependence, this result differs from the FN factor not only quantitatively but qualitatively. Distinctions between exponential factors in the quantum and semiclassical description of tunneling through the triangular barrier are exposed in the following expression

$$T(E) \sim \begin{cases} \exp[-4(E - \overline{eV}/2)^{3/2}/(3\mathcal{F})], & eV \le E_{bw}^0, \\ \exp[-4(E + \overline{eV}/2)^{3/2}/(3\mathcal{F})], & eV > E_{bw}^0, \end{cases} \quad \textbf{(12)}$$

which is valid under the just-mentioned restrictions. As seen from Eq. (12), for a fixed energy and at low voltages, the exponent *decreases* with the field strength *increase* (though, not in the way predicted by the semiclassical approximation). At high voltages, however, the exponent *decrease* begins to *increase* at field strength $\mathcal{E}_{\rm cr} = 4(E - E^0_{bw}/2)/(\mathcal{N}- 1)$. Above this value, the through *sls* band tunneling is no longer enhanced by the electric field; the field effect on tunneling is just the opposite. It is worth stressing that for energies of the order of E^0_{bw} (most interesting), $\mathcal{E}_{\rm cr} \ll 1$, that is well below the level spacing that would be comparable with zero-field bandwidth. In the latter case, the field-suppressing effect on tunneling is expected from elementary physical considerations.[15]

V. TUNNELING THROUGH WS BAND

Similarly to the treatment of the *sls* band, excluding the small energy interval close to the top of WS band, $E < \overline{\rm eV}/2 - \mathcal{E}$, for large $\mathcal{N}$, the energy and field dependence of ratio (2) is determined by

$$\mathcal{D}_{\mathcal{N}}(E)G_{\mathcal{N}\mathcal{N}}(E) \approx \frac{\mathcal{E}/\pi}{\sqrt{\sinh\delta\sinh\delta'}} \times\left\{-\frac{1}{2}\exp\left[\frac{2}{\mathcal{E}}(\Phi_\delta - \Phi_{\delta'}) + \delta\right]\cos\frac{\pi E}{\mathcal{E}} + \exp\left[\frac{2}{\mathcal{E}}\Phi_\delta + \Phi_{\delta'} + \delta\right]\sin\frac{\pi E}{\mathcal{E}}\right\}, \tag{13}$$

and by the symmetry of the Green function matrix elements. In Eq. (13), $2\cosh\delta' = {\rm eV}/2 - E$, and $\Phi_{\delta'} = \delta'\cosh\delta' - \sinh\delta'$.

On the other hand, the eigenenergies within the WS band are subject to the solution of the following equation[6]

$$\sin\frac{\pi E}{\mathcal{E}} = \frac{1}{2}\exp\left(-\frac{4}{\mathcal{E}}\Phi_{\delta'} - 2\delta'\right)\cos\frac{\pi E}{\mathcal{E}}. \tag{14}$$

The use of relations (13) and (14) in Eq. (2) yields

$$T(E) \sim \frac{\sinh\delta}{\sinh\delta'}\exp[-2(\delta - \delta')]\exp\left(-\frac{4}{\mathcal{E}}\Phi^-\right), \tag{15}$$

with $\Phi^- = \Phi_\delta - \Phi_{\delta'}$. And for energies $E_n = (n + 1/2)\,\mathcal{E}$, that is, between the WSL energies, we have from Eq. (13)

$$T(E) \sim \sinh\delta\,\sinh\delta'\exp(-2\delta)\exp\left(-\frac{4}{\mathcal{E}}\Phi^+\right), \tag{16}$$

where $\Phi^+ = \Phi_\delta + \Phi_{\delta'}$.

The preceding derivation has been performed for odd values of $\mathcal{N} = 2N + 1$. The obtained result does not depend on the crystal thickness other than through eV, implying its independence of $\mathcal{N}$ parity.

FIGURE 2 shows that the energy dependence expressed in Eq. (15) envelopes the oscillatory behavior of $T(E)$. The latter is calculated from Eqs. (2) and (3). It also demonstrates that, except near the WS-band edge, Eq. (15) reproduces maxima of tunneling probability that are attained at the WSL energies $E_n = n\mathcal{E}$ ($\mathcal{N} = 2N + 1$) $n = 0, 1, 2, \ldots$. [For even values of $\mathcal{N}$, $E_n = (n + 1/2)\mathcal{E}$.] The energy dependence obtained in Eq. (16) gives an envelope of the tunneling probability minima. The strict solution of a related scattering problem[12] refers these findings to the case of weak coupling to the leads.

A large difference between the maxima and minima envelopes of $T(E)$ (in the middle of the WS band) is almost entirely determined by the difference between functions $\Phi^-$and Φ^+ [see Eqs. (15) and (16)]. At $E = 0$ the functions Φ_δ and $\Phi_{\delta'}$ are equal. Hence, $\Phi^- = 0$ and $\Phi^+ = 2\Phi_\delta^{\min}$ (minimal and maximal values of Φ_δ, $\Phi_\delta^{\min}$, and $\Phi_\delta^{\max}$, are defined in the legend for FIGURE 3). With the increase of E, Φ_δ decays to zero value at the top of the WS band $E_{\mathrm{WS}}^t = \overline{\mathrm{eV}}/2$. In contrast, Φ_δ monotonously increases up to $\Phi_\delta^{\max}$. So, at the top of the WS band, $\Phi^+ = \Phi^- = \Phi_\delta^{\max}$. For some values of the applied voltage the dependence of functions Φ_δ and $\Phi_{\delta'}$ on energy is illustrated in FIGURE 3.

The extremely sharp resonance structure of tunneling probability exhibited in FIGURE 2 has the same nature as the well-known phenomenon of resonance tunneling through a barrier–well–barrier structure. In the given case, the potential profile of the left $[U_n^{\mathrm{l}}(E)]$ and right $[U_n^{\mathrm{r}}(E)]$ barriers is such that $U_n^{\mathrm{l}}E = U^{\mathrm{r}}_{\mathcal{N}+1-n}(-E)$ (inverted triangular barriers). Therefore, if the energy shifts from the value $E = 0$, at which the structure is totally symmetric (the tunneling probability is equal or close to unity for odd and even $\mathcal{N}$, respectively), the maxima of transmission are more strongly suppressed for larger energies because of increasing system asymmetry. In contrast, the dependence of $T(E)$ minima on energy is much weaker, because the total length of two barriers is energy independent.

As in the case of through *sls* band tunneling, explicit expressions of Φ_δ and $\Phi_{\delta'}$ as functions of energy can be given at energies $\overline{\mathrm{eV}}/2 - E \ll 1$. For Φ_δ, there is an additional restriction on the applied voltage $\overline{\mathrm{eV}}/4 - E \ll 1$. Under the conditions just indicated, $3\Phi_\delta \approx (\overline{\mathrm{eV}}/2 + E)^{3/2}$ and $3\Phi_{\delta'} \approx (\overline{\mathrm{eV}}/2 - E)^{3/2}$ [compare to Eq. (12)]. It is seen that with these definitions of $\Phi_\delta(\delta')$, the requirements $\Phi^- = 0$, $\Phi^+ = 2\Phi_\delta^{\min}$ at $E = 0$, and $\Phi^+ = \Phi^- = \Phi_\delta^{\max}$ at $E = \overline{\mathrm{eV}}/2$ are met. Moreover, for the values of $\overline{\mathrm{eV}}$ comparable with the zero-field bandwidth, the approximate dependencies reasonably reproduce the behavior of exact functions Φ_δ and $\Phi_{\delta'}$ in the entire WS band (see FIG. 3).

VI. CONCLUSION

We have found explicit expressions of the exponential factors that govern tunneling probability through a tilted tight-binding band. At high voltages, we predict specific field effects on tunneling through the *sls* and WS bands. Probably, the most suitable technique for their observation is suggested by ballistic-electron-emission microscopy,[16] which enables a direct probing of the energy dependence of electron transmission.

The formalism used is not applicable for extended states assisted tunneling. It also cannot be used to describe the resonance structure of the tunneling probability within any of the characteristic bands. As is emphasized earlier, to consider these issues, the corresponding scattering problem has to be solved (in focus elsewhere[12]). Nevertheless, because of its simplicity, the suggested evaluation of the tunneling exponential factor is certainly a useful approach, especially for more complex effects, such as, for example, Zener tunneling.

From the experimental point of view, the obtained results first of all address the tunneling mechanism of electrical breakdown in ultrathin dielectric layers in solids. As such, they contribute to our understanding of the possible thickness limits of efficient electron tunneling that are currently the source of significant research and debate.[17] Not to forget obvious links of these results with fundamental effects of Zener tunneling, Franz-Keldysh effect, and a number of related phenomena.

ACKNOWLEDGMENTS

This work was supported by Swedish Research Council for Engineering Sciences (TFR). Partial support from INTAS under grant 99-864 is acknowledged.

REFERENCES

1. WANNIER, G.H. 1960. Phys. Rev. **117:** 432; 1962. Rev. Mod. Phys. **34:** 645 (1962).
2. MENDEZ, E.E. & G. BASTARD. 1993. Phys. Today **46**(6): 34); ROSSI, F. 1998. Semicond. Sci. Technol. **13:** 147; LEO, K. 1998. *ibid.* **13:** 249; see also MADISON, K.W., M.C. FISHER & M.G. RAIZEN. 1999. Phys. Rev. A **60:** R1767 (for recent progress in the experiment on optically driven lattices).
3. DI CARLO, A., P. VOGL & W. PÖTZ. 1994. Phys. Rev. B **50:** 8358.
4. LINDER, N. *et al*. 1995. Phys. Rev. B **52:** 17352.
5. HACKER, K. & G. OBERMAIR. 1970. Z. Phys. **234:** 1; SAITOH, M. 1973. J. Phys. C: Solid State Phys. **6:** 3255; STEY, G.C. & G. GUSMAN. 1973. J. Phys. C: Solid State Phys. **6:** 650; FUKUYAMA, H., R.A. BARI & H.C. FOGEDBY. 1973. Phys. Rev. B **8:** 5579.
6. ONIPKO, A. & L. MALYSHEVA. 2001. Solid State Commun. **118:** 63; 2001. Phys. Rev. B **63:** 235410 .
7. ZENER, C. 1934. Proc. R. Soc. **145:** 523.
8. FRANZ, Z. 1958. Naturforsch. Teil A **13:** 484; KELDYSH, L.V. 1958. Zh. Eksp. Teor. Fiz. **34:** 1138 [Sov. Phys. JETP **34:** 788].
9. DATTA, S. 1995. Electronic Transport in Mesoscopic Systems. Cambridge University Press. Cambridge.
10. MALYSHEVA, L.I. 2000. Ukr. Fiz. Zh. **45:** 1475.
11. ABRAMOWITZ, M. & I.A. STEGUN. 1965. Handbook of Mathematical Functions. Dover. New York.
12. ONIPKO, A. & L. MALYSHEVA. 2001. Phys. Rev. B **64:** 195131.
13. FOWLER, R.H. & L. NORDHEIM. 1928. Roy. Soc. Proc. A **119:** 173.
14. Simmons, J.G. 1963. J. Appl. Phys. **34:** 1793.
15. DAVIES, J.H. 1998. The Physics of Low-Dimensional Semiconductors. Cambridge University Press. Cambridge.
16. SMITH, D.L. & S.M. KOGAN. 1996. Phys. Rev. B **54:** 10354, and references therein.
17. Kingon, A.I., J.-P. Maqria & S.K. Streiffer. 2000. Nature **406:** 1032.